encit 2020

ABCM Associação Brasileira de Engenharia e Ciências Mecânicas

18th Brazilian Congress of Thermal Sciences and Engineering
November 16-20, 2020 (Online)

ENC-2020-0547
ACADEMIC SCRAMJET DESIGN TO FLIGHT AT 20 KM OF ALTITUDE AT MACH NUMBER 5.79 INTEGRATED AT ROCKET ENGINE S30

Lucas de Almeida Sabino Carvalho
Luísa Mirelle Costa dos Santos
José Fernandes Filho
Pedro Paulo Batista de Araújo
Universidade Federal do Rio Grande do Norte/UFRN - Centro de Tecnologia. Av. Senador Salgado Filho, 3000 - Campus Universitário, Lagoa Nova CEP 59.078-970 – Natal/RN – Brasil
carvalholucas01@hotmail.com, luisasantos98@hotmail.com, josef1703@hotmail.com, araujo.projects@gmail.com

José Bismark de Medeiros
Universidade Federal do Vale do São Francisco/UNIVASF –Colegiado Acadêmico de Engenharia Mecânica. Campus Juazeiro. Av.Antonio Carlos Magalhães, 510–Santo Antonio. CEP 48.902-300 - Juazeiro, BA- Brasil
jose.bismark@univasf.edu.br

Paulo Gilberto de Paula Toro
Universidade Federal do Rio Grande do Norte/UFRN - Centro de Tecnologia. Av. Senador Salgado Filho, 3000 - Campus Universitário, Lagoa Nova CEP 59.078-970 – Natal/RN – Brasil
toro11ptoro@gmail.com

Abstract. *The design of an academic symmetric planar scramjet is developed by undergraduate and graduate students from Universidade Federal do Rio Grande do Norte (UFRN), to demonstrate the supersonic combustion, at 20 km of altitude with Mach number 5.79, integrated as payload of Brazilian rocket engine S30. To design the academic scramjet, analytical approach, considering air as an ideal gas and no viscous effects, is applied. The airflow properties (pressure, temperature, density and Mach number), from leading-edge to trailing-edge of the scramjet vehicle, are presented for power-off (without burning hydrogen fuel) and power-on (burning hydrogen as heat addition assumption) to academic symmetric planar scramjet. Also, a numerical analysis of the scramjet in power-off configuration is presented, using ANSYS Fluent code, to evaluate the accuracy of analytical design. Finally, the thrust is showed considering power-o of and power-on conditions.*

Keywords: *scramjet, hypersonic airbreathing propulsion, hypersonics, analytical analysis, aerospace.*

1. INTRODUCTION

There is a constant search for improvements in technologies for access to space, leading to enhancement of known technologies and development of new ones. One technology that is being a topic of worldwide interest is on hypersonic flight, were several countries are acting on research and development of the hypersonic vehicles called scramjet. NASA X-43 scramjet hypersonic vehicle, that flew at Mach numbers 7 and 10, burning hydrogen for about 10 seconds; or U.S. Air Force X-51 scramjet hypersonic missile, at Mach Number 5 burning hydrocarbon for about 150 seconds.

In Brazil, research in scramjet vehicles are being conducted in Laboratório de Aerotermodinâmica e Hipersônica Prof. Henry T. Nagamatsu, at Instituto de EstudosAvançados (IEAv) since 2007, proposed to design, to develop, to manufacture a technological scramjet to demonstrate, the supersonic combustion (Fig. 1), in free flight in about 30 km of altitude, at hypersonic speed, corresponding to the Mach number 10 (Rolim et. al, 2009).

Researches in hypersonic and scramjet are also being conducted at Universidade Federal do Rio Grande do Norte (UFRN) by undergraduate and graduate students.

A scramjet vehicle is a variation of ramjet, in which the flow entering the combustion chamber is in supersonic. The scramjet, as sharp cones or wedges, in hypersonic flight, uses the oblique shockwave phenomena, to promote compression and deceleration of the flow to the combustion chamber (Fig. 2).

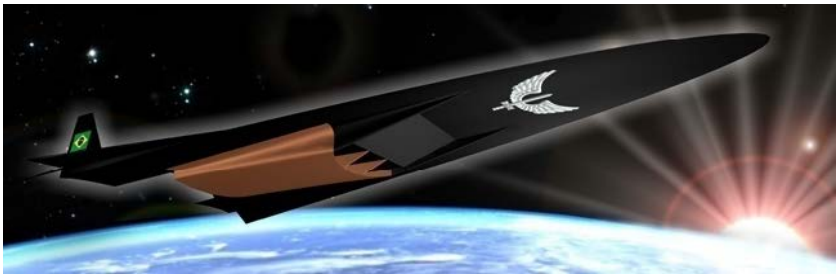

Figure 1. Scramjet 14-X waverider.

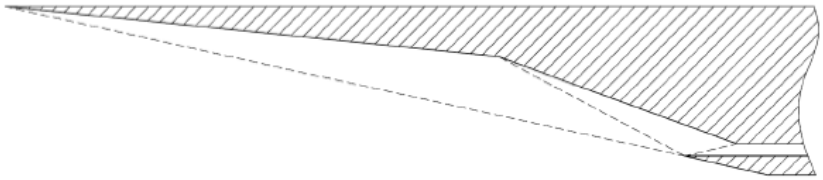

Figure 2. Oblique shockwaves in a scramjet vehicle.

The main advantage of a scramjet engine is the provide thrust effectively in hypersonic flight (Curran, 2001), also being an alternative for saving weight for certain stages in atmospheric flight, since it requires less amount of fuel than standard rocket engines. Scramjet is a highly integrated system, where engine and vehicle are indistinguishable. It can only be activated in hypersonic regime, which means it needs to be accelerated until reach the required velocity, therefore, being integrated to a rocket vehicle until reach the Mach number needed to start the supersonic combustion.

The terminology for scramjet was defined by Heiser and Pratt (1994), that divided scramjet in three parts and several stations (Fig. 3), which are external (stations 0 to 1, governed by incident shock waves) and internal (stations 1 to 3, governed by reflected shock waves) compression section (inlet), combustion chamber (combustor, stations 3 to 4, governed by one-dimensional flow with heat addition, Rayleigh flow) and internal (stations 4 to 9) and external (stations 4 to 10) expansion section (outlet, governed by Prandtl-Meyer expansion wave theory and area ratio).

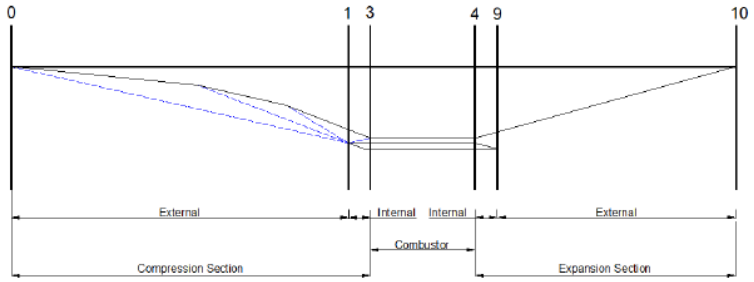

Figure 3. Scramjet terminology (Adapted from Heiser and Pratt, 1994).

In this work, it is proposed the design of an academic scramjet to be flying at altitude of 20 km with Mach number 5.79, integrated to the Brazilian rocket engine S30 to first stage flight. The analysis was done analytically, without considering viscous effects, for power-off (no heat addition) and power-on (with heat addition) configurations.

2. METHODOLOGY

Analytical methodology was used to determine the thermodynamic properties (pressure, temperature, and density), speed of sound and Mach number for the scramjet. By closed form relationships, it is possible to determine the flow properties by the theories of oblique shock waves, one-dimensional flow with heat addition, expansion waves and area ratio integrated, respectively, for scramjet compression, combustion chamber and expansion sections. The same flow considerations for analytical analysis were considered to the numerical analysis carried out by ANSYS Fluent code.

For this work, air behaves as a calorically perfect gas and the viscous effects are not considered for one-dimensional flow at the streamlines from the leading-edge to trailing-edge of the scramjet vehicle, in hypersonic flight at Mach number 5.79, at the altitude of 20 km (Table 1).

Table 1. Aerothermodynamic properties at 20 km of altitude (Adapted from NASA, 1976).

Temperature [K]	pressure [kPa]	density [kg/m³]	speed of sound [m/s]
216.65	5.529	0.0889	295.06

2.1 **Governing equations**

For the compression section, since the scramjet is design as a sharp edge, it leads to the formation of oblique shockwaves. Anderson (1990) presents the main equations to compute the ratios of thermodynamic properties and Mach number after an oblique shockwave, shown below (Fig. 4). The subscript in/out denotes the properties before and after the shockwave.

$$M_{out} = \sqrt{\frac{(M_{in}\,sen\beta)^2+\frac{2}{(\gamma-1)}}{\frac{2\gamma}{(\gamma-1)}(M_{in}\,sen\beta)^2-1}} \tag{1}$$

$$\frac{p_{out}}{p_{in}} = 1+\left[\frac{2\gamma}{(\gamma-1)}(M_{in}sen\beta)^2-1\right] \tag{2}$$

$$\frac{\rho_{out}}{\rho_{in}} = \frac{(\gamma+1)(M_{in}\,sen\beta)^2}{(\gamma-1)(M_{in}\,sen\beta)^2+2} \tag{3}$$

$$\frac{T_{out}}{T_{in}} = \frac{\frac{p_{out}}{p_{in}}}{\frac{\rho_{out}}{\rho_{in}}} = \left[1+\left[\frac{2\gamma}{(\gamma-1)}(M_{in}sen\beta)^2-1\right]\right]\left[\frac{(\gamma+1)(M_{in}\,sen\beta)^2}{(\gamma-1)(M_{in}\,sen\beta)^2+2}\right] \tag{4}$$

where, M, p, ρ, T, γ, β are Mach number, pressure, temperature, ratio of specific heats, and the shock wave angle. The shockwave angle β is related to the Mach number and sharp edge angle θ by Eq. (5) shown as

$$tg(\theta) = 2cotg(\beta) = \left[\frac{(M_{in}\,sen\beta)^2-1}{M_{in}^2(\gamma+cos2\beta)+2}\right] \tag{5}$$

The hypersonic flow is redirected after the oblique shock waves (Fig. 4) to be parallel the scramjet surface due to the sharp edge angle, increasing the airflow properties and decelerating it to supersonic speeds (Anderson, 1990).

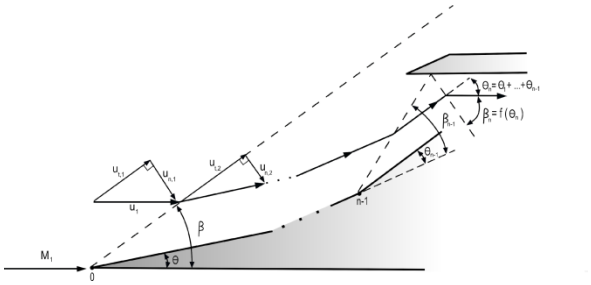

Figure 4. Incident and reflected oblique shockwaves.

For several ramps, the reflection angle can be related to the angle of previous ramps by the equation

$$\theta_{reflected} = \theta_1+\theta_2+\cdots+\theta_n \tag{6}$$

where, $\theta_{reflected}$ is the reflection angle, θ_n the angle of the nth ramp, and n is the number of ramps, at the external section (Fig. 3).

To consider the combustion effects, the analysis of the scramjet combustor is done using Rayleigh flow theory, which states a one-dimensional flow with constant area and heat addition (Anderson, 1990).

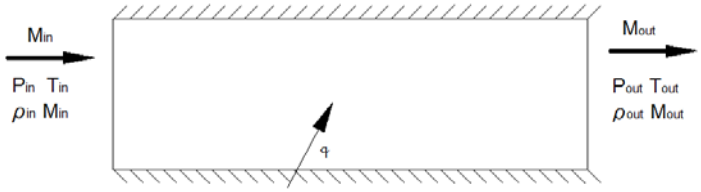

Figure 5. Rayleigh flow illustration (Adapted from Anderson, 1990).

For Rayleigh flow, the heat added to the flow, to simulate the combustion process inside scramjet combustion chamber, is defined as

$$q = \dot{m}_0 c_p \left(T_{0,out} - T_{0,in}\right) \tag{7}$$

where, q is the heat added, $\dot{m}_0$ the mass flow rate, c_p the specific heat at constant pressure, $T_{0\,out}$ the total temperature on the exit of the combustor and $T_{0\,in}$ the temperature on the entry of the combustor. The total temperature can be related with Mach number and static temperature by

$$\frac{T_0}{T} = 1 + \frac{1-\gamma}{2} M^2 \tag{8}$$

The ratios of thermodynamic properties in Rayleigh flow considering heat addition and one-dimensional flow are defined as

$$\frac{p_{out}}{p_{in}} = \left(\frac{1+\gamma M_{in}^2}{1+\gamma M_{out}^2}\right) \tag{9}$$

$$\frac{\rho_{out}}{\rho_{in}} = \left(\frac{1+\gamma M_{out}^2}{1+\gamma M_{in}^2}\right)\left(\frac{M_{in}}{M_{out}}\right)^2 \tag{10}$$

$$\frac{T_{out}}{T_{in}} = \frac{\frac{P_{out}}{P_{in}}}{\frac{\rho_{out}}{\rho_{in}}} = \left(\frac{1+\gamma M_{in}^2}{1+\gamma M_{out}^2}\right)^2 \left(\frac{M_{out}}{M_{in}}\right)^2 \tag{11}$$

$$\frac{T_{0,out}}{T_{0,in}} = \left(\frac{1+\gamma M_{in}^2}{1+\gamma M_{out}^2}\right)^2 \left(\frac{M_{out}}{M_{in}}\right)^2 \left(\frac{1+\frac{\gamma-1}{2}M_{out}^2}{1+\frac{\gamma-1}{2}M_{in}^2}\right) \tag{12}$$

For expansion section, the calculations were done using the area ratio formulation (Heiser and Pratt, 1994), which relates the entry and exit area of the expansion section of a scramjet by Eq. (13)

$$\frac{A_{out}}{A_{in}} = \frac{M_{in}}{M_{out}} \left(\frac{1+\frac{\gamma-1}{2}M_{out}^2}{1+\frac{\gamma-1}{2}M_{in}^2}\right)^{\frac{\gamma+1}{2*(\gamma-1)}} \tag{13}$$

The ratios of thermodynamic properties for the expansion section are defined as

$$\frac{T_{out}}{T_{in}} = \left(\frac{1+\frac{\gamma-1}{2}M_{in}^2}{1+\frac{\gamma-1}{2}M_{out}^2}\right) \tag{14}$$

$$\frac{P_{out}}{P_{in}} = \left(\frac{T_{out}}{T_{in}}\right)^{\frac{\gamma}{\gamma-1}} \tag{15}$$

$$\frac{\rho_{out}}{\rho_{in}} = \frac{\frac{P_{out}}{P_{in}}}{\frac{T_{out}}{T_{in}}} = \left(\frac{T_{out}}{T_{in}}\right)^{\frac{1}{\gamma-1}} \tag{16}$$

Applying oblique shock waves, heat addition on one dimensional (Raleigh) flow and area ratio theories; it is possible to obtain the thermodynamic properties, speed of sound and Mach number for scramjet vehicle design, from leading-edge to trailing-edge, flying at 20 km altitude and Mach number 5.79.

It was calculated the thrust generated by power-off and power-on configurations by the methodology presented by Heiser and Pratt (1994), which considers the entire control volume from compression to expansion region.

$$F = \dot{m}_{10}u_{10} - \dot{m}_0 u_0 + (p_{10} - p_0)A_{10} \tag{17}$$

where, F is the not-installed thrust, $\dot{m}_{10}$and $\dot{m}_0$is the mass flux at expansion and compression section,u_{10} and u_0 the velocity at expansion and compression section, p_{10} and p_0 is the pressure at expansion and compression section, and A_{10} the area of expansion section. Drag force is not considered in this calculation.

2.2 **Computational Fluid Dynamics**

For the Computational Fluid Dynamics analysis, the airflow was considered air as calorically perfect, and without viscous effects, to compare with the analytical design with same assumptions. The comparison was done with power-off configuration, without combustion, to simplify the analysis.

The mesh is considered as good quality for skewness lower than 0.95 and minimum orthogonal quality of 1. The quality mesh used was skewness 0.29 and minimum orthogonal was 0.89, and the mesh was structured, where mesh cells are aligned with the flow, with 160486 elements to lower computational effort and better results.

The simulation was done with the second order upwind scheme, as this scheme computes the results with higher accuracy than the first order upwind scheme. The inviscid solver was used to solve the Euler equations, in which momentum and energy equations are reduced due absence of molecular diffusion (ANSYS, 2013).

$$\frac{\partial \rho}{\partial t} + \nabla \cdot (\rho \vec{v}) = S_m \tag{18}$$

$$\frac{\partial}{\partial t}(\rho \vec{v}) + \nabla \cdot (\rho \vec{v}\vec{v}) = -\nabla p + \rho \vec{g} + \vec{F} \tag{19}$$

$$\frac{\partial}{\partial t}(\rho E) + \nabla \cdot \left(\vec{v}(\rho E + p)\right) = -\nabla \cdot \left(\sum_j h_j J_j\right) + S_h \tag{20}$$

where,ρ is the fluid density, $\vec{v}$ the flow velocity vector, p the pressure, $\vec{g}$ the gravity acceleration, $\vec{F}$ the external body forces, S_m is the mass added to the continuous phase from the dispersed second phase and user defined sources, E is the total energy, J_j is the diffusion flux of j species, and S_h includes the chemical reaction heat and any others user-defined heat sources.

3. RESULTS

The aero-thermo-dynamic properties over the sections of the scramjet allow not only to obtain the scramjet dimensions and to integrate as payload at S30 rocket engine, but also to study the influence of burning hydrogen (simulated by heat addition) on scramjet thrust by comparing power-off and power-on configurations.

Considering the analytical analysis, one may observe the thermodynamic properties behavior in every section of the scramjet (Table 2). The airflow property (pressure, temperature, and density) ratios are constant through the external section, therefore the external section is optimized by the same shook wave strength (Ran and Mavris, 2005) guaranteeing shock on-lip and shock on-corner criteria.

Table 2. Compression (external and internal) section results.

	Units	Freestream	Ramp 7.25°	Ramp 8.6°	Ramp 10.3°	Reflection
M_{in}		5.79	5.79	4.87	4.04	3.29
θ_{in}	°	-	7.25	8.6	10.3	26.15
β_{out}	°	-	15.38	18.41	22.36	43.467
M_{out}		-	4.87	4.04	3.29	1.81
p_{out}/p_{in}		-	2.59	2.59	2.59	5.82
T_{out}/T_{in}		-	1.34	1.34	1.34	1.92
ρ_{out}/ρ_{in}		-	1.93	1.92	1.92	3.04
P_{out}	Pa	5529.38	14316.27	37078.71	96016.93	559268.09
T_{out}	K	216.65	291.38	391.94	527.17	1010.034
ρ_{out}	kg/m^3	0.089	0.1711	0.3296	0.6346	1.9293
a_{out}	m/s	295.04	342.16	396.84	460.23	637.04
u_{out}	m/s	1709.64	1665.41	1603.21	1516.07	1152.56
T_{total}	K	1671.53	1671.96	1671.34	1671.26	1671.26

Also, the total temperature through external (all incident shock waves) and internal (reflected shock wave) compression are constants, so the energy is conserved. The airflow property (pressure, temperature, and density) increase and airflow velocity (and corresponding Mach number) decrease through the compression (external and internal) section, from the leading-edge to the combustion chamber. Finally, the temperature of 1010 K and supersonic Mach number of 3.29 at the entrance of the combustion chamber are adequate to burning hydrogen in supersonic combustion condition.

The combustion chamber entrance conditions is the same values of conditions after the reflected shock wave, and the exit combustion chamber conditions is the same as the entrance of the combustion chamber conditions, since there is no burning of hydrogen at the combustion chamber. Also, the airflow condition at the entrance of expansion section is the same values of the exit of the combustion chamber (Table 3). Applying area ratio theory, one may divide the expansion section length and determine the airflow properties through the expansion section (Table 3). As one may see, the total temperature through expansion (internal and external) section is conserved. Finally, the airflow property (pressure, temperature, and density) decreases, and airflow velocity (and corresponding Mach number) increases through the (internal and external) expansion section, from the combustion chamberto the trailing-edge.

Table 3. Combustion chamber section and expansion (internal and external) section results, power-off, no hydrogen burning.

	Units	Combustion chamber entrance (from reflected shock wave)	Entrance of the expansion section (same combustion chamber exit)	Expansion section
M		1.81	1.81	5.592
p	Pa	559268.09	559268.09	3169.98
T	K	1010.03	1010.03	230.38
ρ	kg/m^3	1.9293	1.9293	0.0479
a	m/s	637.049	637.049	304.25
u	m/s	1152.563	1152.563	1701.38
T_{total}	K	1671.26	1671.26	1671.26

Applying the ANSYS fluent code, one may observe the same behavior as analytical analysis from leading-edge to the trailing-edge of the scramjet. Airflow (pressure, temperature, and density) properties increase at the compression section, remain constant at the combustion chamber (because there is no hydrogen burning), and decrease at the expansion section (Figs. 6 to 8). However, the airflow velocities (and corresponding Mach number) decrease at the compression section, remain constant at the combustion chamber, and increase at the expansion section (Fig. 9). One may divide the expansion section in many subdivisions as desired (in present case was 10 subdivisions).

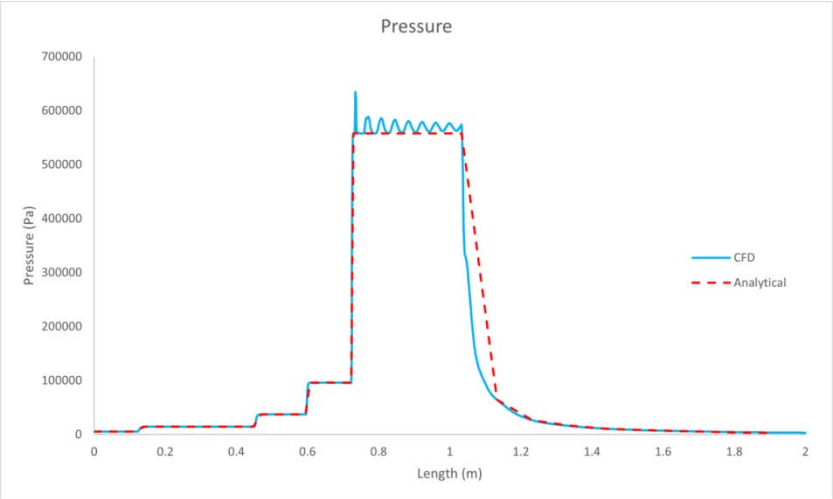

Figure 6. Pressure profiles.

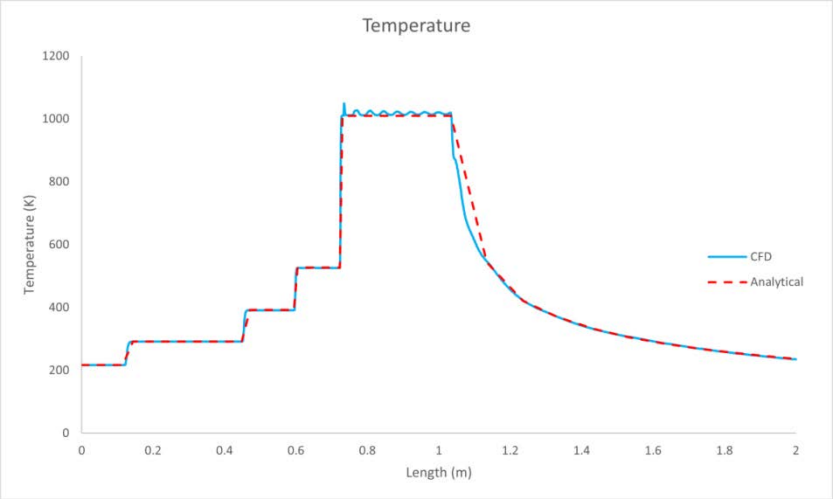

Figure 7. Temperature profiles.

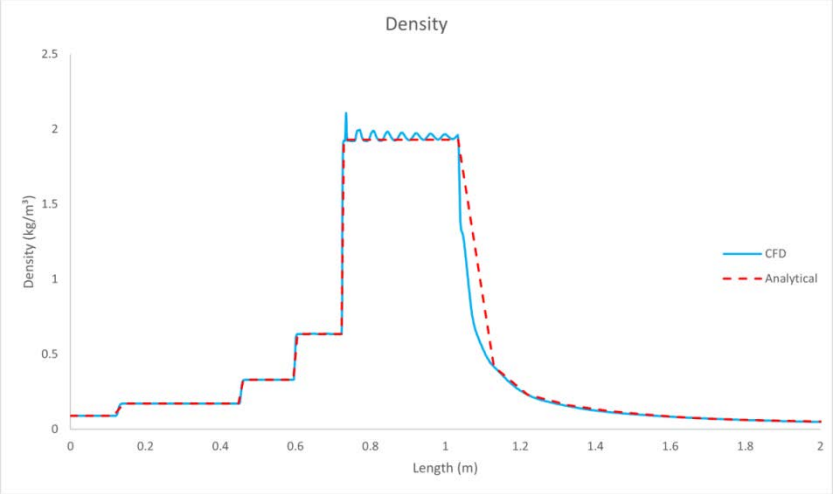

Figure 8. Density profiles.

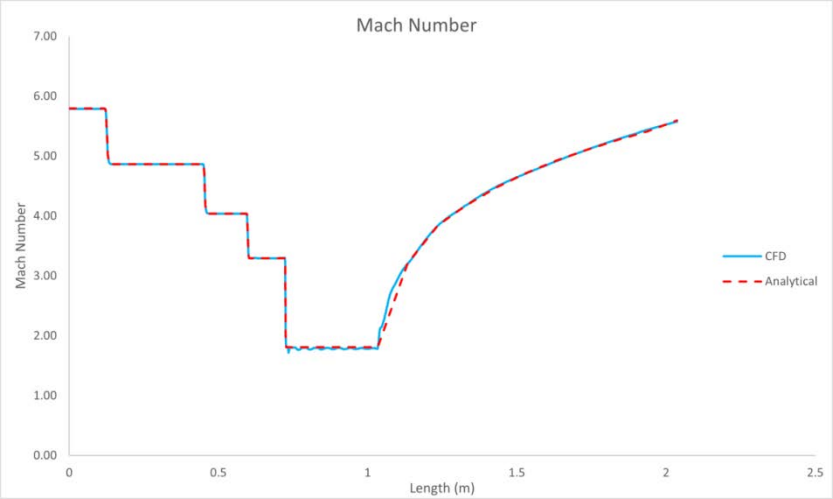

Figure 9. Mach number profiles.

The pressure, temperature, density, and Mach number contours are presented for completeness (Figs. 10 to 13). As one may observe, the shock on-lip and shock on-corner are satisfied, since all incident shockwaves are incident at the leading-edge of the cowl, and the reflected shockwave incident at the entrance of the combustion chamber. Also, the

pressure, temperature, density contours show the airflow properties increase at the compression section, remain constant at the combustion chamber, and decrease at the expansion section, and the airflow velocities have the contrary effects.

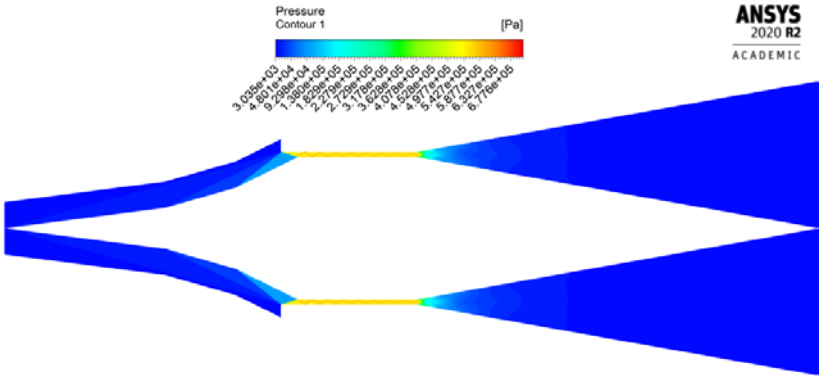

Figure 10. Pressure contour

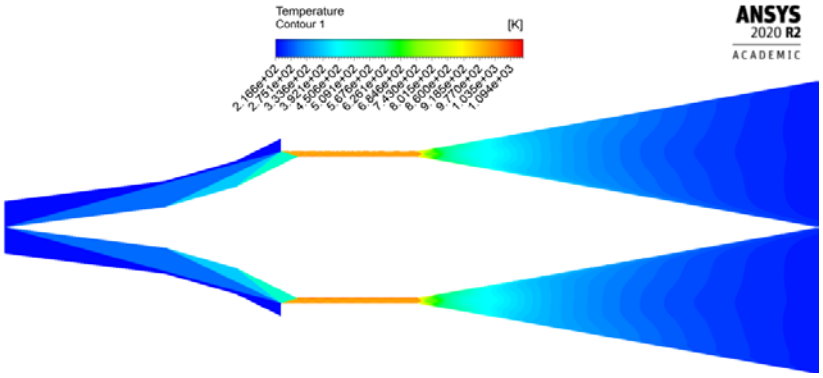

Figure 11. Temperature contours.

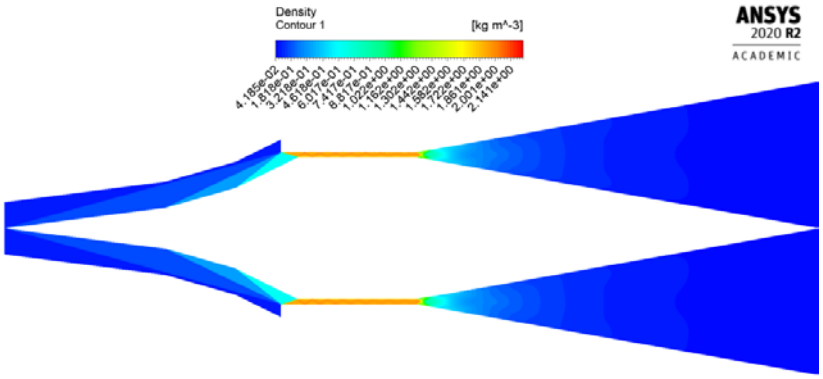

Figure 12. Density contours.

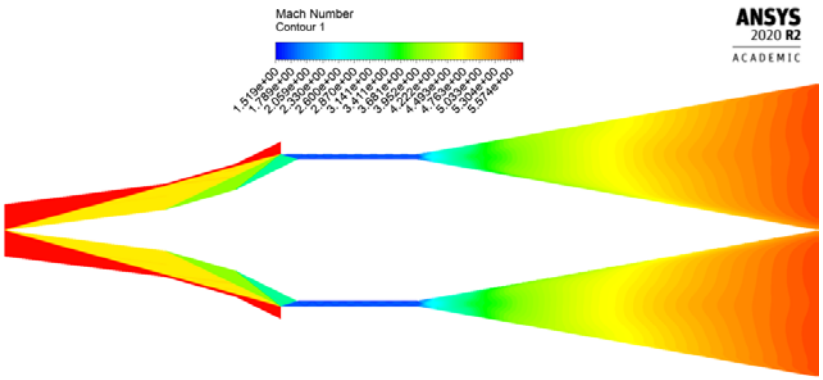

Figure 13. Mach number contours.

For power-on, the conditions on compression section are the same conditions of power-off (Tab. 2). Considering the combustion of hydrogen and air are burning at supersonic velocity, it is assumed the Mach number at the combustion chamber exit is 1.1.

One may observe, on the combustion chamber section, the thermodynamic properties (pressure, temperature, density and sound speed) increase, and combustion products velocity decreases, due to the Mach number of 1.1 assumed. On the other hand, at the expansion section, the thermodynamic (pressure, temperature, density and sound speed) decrease, and the combustion products velocity increase, to Mach number of 5.119, lower than the scramjet flight Mach number of 5.79 (Tab. 4). Therefore, one may expect, heat addition on one-dimensional flow is not a good approach to simulate the burning of hydrogen and air in supersonic velocity, or even burning hydrogen and air in supersonic velocity (heat addition) there is no possibility to use of supersonic combustion to produce thrust (Tab. 4).

However, as one may observe, the Eq. 17 shows the thrust is due to velocity, not the Mach number. Mach dimensionless number is not representative of the flow parameter (Tab. 4).

The generated thrust was calculated using the methodology presented by Heiser and Pratt (1994), with power-off and power-on being compared. The power-off configuration presented a generated thrust of -390.83 N, what demonstrates a gradual reduction over scramjet velocity, whereas power-on configuration has a generated thrust of 1638.85 N, demonstrating the efficiency of supersonic combustion to be used as airbreathing propulsion for aerospace vehicle to flight at hypersonic velocity, in the Earth's dense atmosphere.

Table 4. Combustion chamber section and expansion (internal and external) section results with heat addition.

	Units	Combustor entrance	Combustor exit (with heat)	Expansion section (with heat)
M		1.81	1.1	5.119
p	Pa	559268.09	2401582.33	8444.50
T	K	1010.03	1603.30	319.076
ρ	kg/m^3	1.9293	10.82	0.1910
a	m/s	637.049	802.63	358.05
u	m/s	1152.563	882.89	1832.89
T_{total}	K	1671.26	1991.30	1991.30

4. CONCLUSIONS

The preliminary design, considering airflow as calorically perfect gas and there are no viscous (boundary layer) effects, of a scramjet flying at Mach number 5.79 at 20 km altitude is presented. The airflow properties (pressure, temperature, density and sound velocity) as well as airflow velocities, from the leading-edge to trailing-edge, of the scramjet, are presented, for power-off and power-on conditions.

For power-off conditions, the total temperature remains the same from the leading-edge to trailing-edge, of the scramjet, showing no burning of hydrogen and airflow at the combustion chamber. The airflow properties increase and airflow velocity (Mach number) decreases at the compression section. The airflow properties and airflow velocity (Mach number) remain constant at the combustion chamber, and the airflow properties decrease and airflow velocity (Mach number) increases at the expansion section.

On the other hand, for power-on conditions, the total temperature increases at the combustion chamber due to heat addition, to simulate, the burning of hydrogen and airflow at the combustion chamber. The airflow properties increase and airflow velocity (Mach number) decreases at the compression section. The airflow properties increase and airflow velocity (Mach number) decreases at the combustion chamber and the airflow properties decrease and airflow velocity (Mach number) increases at the expansion section.

The numerical analysis was done, considering power-off condition, in order to validate the analytical methodology applied. Numerical simulation allows observing airflow behavior from the leading-edge to trailing-edge, of the scramjet.

5. ACKNOWLEDGEMENTS

The Authors would like to thank Universidade Federal do Rio Grande do Norte (UFRN) the support given to complete this scientific work. The last Author (as Visiting Professor) would like to express appreciation to UFRN the possibility to apply the knowledge in aerothermodynamics and hypersonics in the research area in hypersonic airbreathing propulsion based on supersonic combustion ramjet (scramjet) technology. The fourth first Authors would like to thank the UFRN for the opportunity to develop scientific research in the aerospace engineering area. A portion of this effort was supported by the Universidade Federal do Vale do São Francisco (UNIVASF) and the fifth Author would like to express his appreciation. This scientific article was developed during the extension course given by Paulo Gilberto de Paula Toro.

6. REFERENCES

Anderson, J. D., Modern Compressible Flow, The Historical Perspective. McGraw-Hill, Inc., ed. 2nd, 1990.

ANSYS, 2013. "Fluent Theory Guide", Ansys Inc, Canonsburg, Washington.

Araújo, J. W. S., *Análise numérica da seção de compressão de demonstrador de tecnologia scramjet*. Undergraduate Conclusion Work, Universidade Federal do Rio Grande do Norte, Natal, Brazil.

Curran, E.T., 2001. "Scramjet Engines: The First Forty Years". AIAA Journal of Propulsion and Power, Vol. 17, n. 6, p. 1138-1148. Nov. - Dez. 2001.

Heiser, W. H.; Pratt, D. T. Hypersonic Airbreathing Propulsion. Washington, D.C, American Institute of Aeronautics and Astronautics, 1994.

Ran, H., and Mavris, D., Preliminary Design of a 2D Supersonic Inlet to Maximize Total Pressure Recovery, 2005.https://doi.org/10.2514/6.2005-7357.

Rolim, T. C., Minucci, M. A. S., Toro, P. G. P. and Soviero, P. A. O., 2009, "Experimental Results of a Mach 10 Conical-Flow Derived Waverider". 16th AIAA/DLR/DGLR International Space Planes and Hypersonic Systems and Technologies Conference. AIAA 2009-7433.

U.S. Standard Atmosphere. NASA TM-X 74335. National Oceanic and Atmospheric Administration, National Aeronautics and Space Administration and United States Air Force. 1976

7. RESPONSIBILITY NOTICE

The authors are the only responsible for the printed material included in this paper.

The authors declare that there is no conflict of interest regarding the publication of this scientific article.